Transactions on Electrical and Electronic Materials (2022) 23:685–692
https://doi.org/10.1007/s42341-022-00405-9

Online ISSN 2092-7592
Print ISSN 1229-7607

REGULAR PAPER

Performance Assessment and Optimization of Vertical Nanowire TFET for Biosensor Application

Parveen Kumar[1] · **Balwinder Raj**[2]

Received: 31 March 2022 / Revised: 26 May 2022 / Accepted: 3 June 2022 / Published online: 27 June 2022
© The Korean Institute of Electrical and Electronic Material Engineers 2022

Abstract

This paper reports the performance assessment of vertical silicon nanowire TFET (V-siNWTFET) design for biosensor applications using dielectric-modulation and gate underlap technique. The sensitivity of the V-siNWTFET is recognizing by immobilizing the different biological molecules such as lipids, biotin, uricase, protein, Gox, streptavidin, uriease, zein etc. in the cavity region which is created under the gate electrode and source oxide. The performance analysis is observed by varying the relative permittivity of the different biomolecules and analyzes the parametric variation both for neutral and charged biomolecules. The sensitivity of the biosensor has been detecting in the terms of drain current (I_D), threshold voltage (V_{TH}), subthreshold slope (SS), transconductance (g_m), and I_{ON}/I_{OFF} ratio. The proposed device structure has capable to reduce the leakage currents and high sensitivity biosensor design in the nanoscale regimes. The obtained best optimum parameters of the proposed devices are I_{ON} (1.37E−08 A/μm), I_{OFF} (9.44E−19 A/μm), SS (29.97 mV/dec) and I_{ON}/I_{OFF} (4.29E+10) ratio with gate work-function ($\phi_{gate} = 4.8$ eV) and uniformly doped (1×10^{-19} cm^{-3}) silicon nanowire at drain to source voltage ($V_{DS} = 1.0$ V). The higher sensitivity of the proposed V-siNWTFET for Biosensor is observed for Zein biomolecules (K = 5).

Keywords Nanowire tunnel FET · Biomolecules · Dielectric modulation · Subthreshold slope · Biosensor · Sensitivity

1 Introduction

As per current situations the whole world suffers from COVID-19 pandemic and continually increase in cases of Omicroon variant is showing the importance of electronic biosensors for the early stage identification of diseases. The biosensor is used for the detection of biomolecules such as lipids, biotin, uricase, protein, Gox, streptavidin, uriease, zein [1–5] etc. and various applications such as food analysis [6], health monitoring [7], detection of crime [8], environmental field [9] etc. In the last decade, field effect transistor (FET) based biosensors [10–15] has been proposed and investigated because of their ability to detect the biomolecules. Apart from this, with the regular shrinking in conventional FET based biosensor devices will leads to deteriorating the device performance in terms of leakage currents, higher subthreshold slope (> 60 mV/dec), short channel effects (SCE) and low I_{ON}/I_{OFF} ratio. The multiple devices such as DGMOSFET, FinFET, CNTFET, Nanowire, Tunnel Field Effect Transistor (TFET) etc. [16–22] has been reported in the literature to immune the SCEs and discover the substitute in terms of low off-state current (I_{OFF}) and minimum subthreshold slope (SS) below the kT/q limit (i.e. SS < 60 mV/decade) and higher I_{ON}/I_{OFF} ratio. Out of these devices, TFET has beem found promising candidate for biosensor application due to its good sensitivity, improved SCEs, energy efficient and proficient to defeat aforesaid issues related to designed FET based biosensors. The operational principal of TFET is based on band-to-band-tunneling (BTBT) and heavily doped p-i-n structure. Due to highly doping concentration in drain as well as source region, it suffers from issue like Random dopant fluctuation (RDFs) which construct the fabrication process complicated and enhance the production cost of the device.

Therefore, junctionless transistor [23] has been explored without junctions in their regions, which makes fabrication process easier because it does not required abrupt doping

✉ Parveen Kumar
parveen.eng@gmail.com

Balwinder Raj
balwinderraj@nitttrchd.ac.in

1 Nanoelectronics Research Lab, Dr. B.R. Ambedkar, National Institute of Technology, Jalandhar 144027, India

2 Department of ECE, National Institute of Technical Teachers Training and Research, Chandigarh 160019, India

profile. Futher to increase the density and scaling probability in the semiconductor devices, Vertical Nanowire TFET structure are preferable because of higher density, electrostatic control on the gate, lower SS and immune to SCEs [24–27]. An exploration is required to check its abiblity for biosensor by the dectection of neutral as well as chargered biomolucules..

In this paper a Vertical Silicon Nanowire TFET (V-siNWTFET) has been proposed for biosensor applications using silicon as the base material of nanowire and dielectric modulation technique. Moreover, performcance assessment has been considered and optimize the device with suitable parameters. A cavity/hole is created on the source-channel interface between the source/gate oxides and electrodes to allow the immobilization of Biomolecules with in the V-siNWTFET. The performance assessment has been observed in the terms of drain currents, SS, transconductance (g_m), I_{ON}/I_{OFF} ratio and their sensitivity, when the biomolecules are enters in the cavity region. The various Biomolecules (neutral as well as charged) has been examined for the performance assesment of V-siNWTFET by their appropriate value of relative permitivity (K). This paper paying attention on required biosensor for commercial medical applications and early detection of dieases which helps to prevents us from the current pandemic.

2 Device Structure and Simuation Framework

In proposed device structure, a uniform highly doped concentration 1×10^{-19} cm^{-3} has been used in all regions of V-siNWTFET by taking silicon material of nanowire in gate-all-around (GAA) environment. The p+source region is framed on silicon substrate (intrinsic type) by utilizing platinum electrode metal workfunction (5.93 eV) and gate metal workfunction (4.8 eV). The work-function of source (ϕ_{source}) always greater than intrinsic silicon (χsi + (Eg/2q) and less than work-function of drain (ϕ_{drain}), where as χsi represents as electron affinity, q shows the charger and Eg taken as energy gap of silicon [28]. The thickness of silicon film has been arranged within Debye-length$\sqrt{\left(\left[(\in_siV_T)/q+60.N\right]\right)}$, whereas V_T,$\in_{si}$, q, N represents as thermal voltage, dielectric constant, charge, carrier-concentration respectively [29].

The proposed device structure of V-siNWTFET is shown in Fig. 1(a). The transfer charaterictics (I_D–V_{GS}) of simulated framework (V-siNWTFET) with respect to reported conventional nanowire TFET [30] as illustrated in Fig. 1(b). The device parameter used for the simulation of V-siNWTFET with conventional NWTFET are gate-lenth = 200 nm, radius of silicon nanowire = 35 nm, gate-oxide thickness = 4.5 nm, workfunction of gate electrode = 4.0 eV with gaussian doping profile = 1×10^{-17} cm^{-3}. The simulation framework place here for V-siNWTFET is exhaustively calibrated with reported work [30] and data has been extracted using plot digitizer tools.

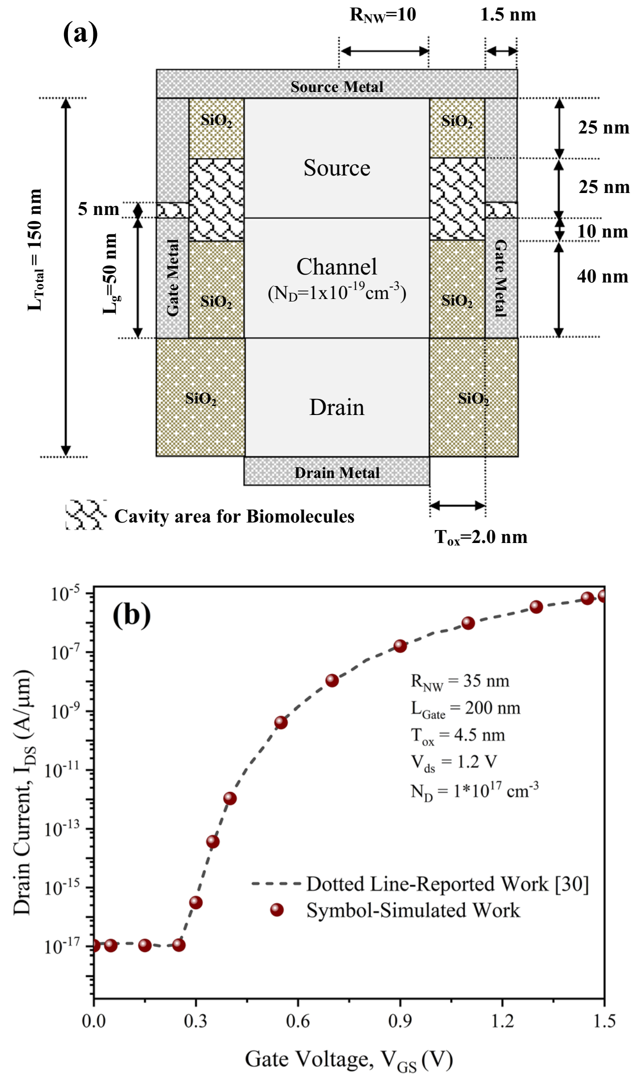

Fig. 1 **a** Cross sectional Two dimestional (2D) viewof propsed JL-NWTFET **b** Calibration Curve (I_D-V_{GS}) with reported work [30]

The optimized parameteric values has been utilized such as gate/channel length (L_{gate} = 50 nm), Cavity length (L_{cavity} = 35 nm), Radius of silicon nanowire (R_{NW} = 10 nm), gate-oxide thickness (T_{ox} = 2 nm), Cavity thikness (T_{cavity} = 2 nm), gate workfunction (ϕ_{gate} = 4.8 eV) and highly doped uniform concentration ($N_D = 1\times10^{-19}$ cm^{-3}) to improve the electrical properties of the device such ON state current (I_{ON}), subthreshold slope (SS), OFF state current (I_{OFF}), Transconductance (g_m) and Sensitivity of the V-siNWTFET.

The detailed device parameters of V-siNWTFET are given in Table 1. The tunneling has been performed through BTBT mechanism at the source-channel interface.

The tunneling current (I_{BTBT}) of the TFET based devices depends upon its tunneling probability of the electrons and engery gap between conduction band (CB) and valance band (VB) which is represents as T(E) and (E_g) respectively. The T(E) is expressed in Eq. (1) and calculated through WKB approximation [31].

$$T(E) \cong exp\left[-\frac{4\lambda\sqrt{2m^*}E_g^{\frac{3}{2}}}{3qh\left(E_g+\Delta\Phi\right)}\right]\Delta\Phi \quad (1)$$

where as E_g denotes the engery gap between CB and VB at tunneling junction, m* shows the effective mass, λ represents the tunneling length and expresses in Eq. (2) [32]

$$\lambda = \sqrt{\frac{\epsilon_{si}}{\epsilon_{bio}}t_{oxt}t_{body}} \quad (2)$$

where as ϵ_{si}, ϵ_{bio}, t_{body} shows the dielectric constant of silicon, dielectric constant of biomolecules and body thickness respectively. The total thickness under the gate is represents as t_{oxt} which is the summation of gate oxide and cavity thickness.

At the thermal equilibrium state, when the gate to source voltage (V_{GS}) is equal to zero and drain-source voltage (V_{DS}) is 1.0 V, device will act as OFF state and engery gap between their bands (conduction band and valence band) will be high. Futher with the increase in V_{GS} from 0 to 1.2 V and V_{DS} still same at 1.0 V, the device will act as ON state and engerygap between conduction band (CB) and valance band (VB) has been reduced. So the tunneling of electrons has possible only in ON state as shown in Fig. 2 because of lesser engerygap between CB and VB. If the engery gap is low, then tunneling probability is higher in case of TFET devices [33].

The cavity area is formed by a adhesion layer in between the source-gate oxides and source-gate electrodes.The biomolecules get immobilized in the cavity area. The total length of the cavity region is taken as 35 nm, out of this 25 nm for source-oxide region and 10 nm for gate-oxide region and $T_{cavity} = 2$ nm has been considered for biomolecules detection. The various biomolecules are immobilization in the cavity area such as Lipids, Biotin, Uricase, Protein, Gox, Streptavidin, Uriease, Zein etc. The simulation of V-siNWTFET is performed by filling biomolecules in the entire cavity area. Intially, the entire cavity is filled by air (K = 1) and the relative permittivity (K) of the biomolecules has been varied from 1.00 to 5.00 for performance assessment of the proposed device. The different models such as Shockley- Read-Hall (SRH) recom5bination model [34], Wentzel-Kramer-Brillouin (WKB) model [35] for numerical yield, Non-local band-to-band-tunneling (BTBT) model for tunneling-probability at the interface [36], bandgap barrowing (BGN) model for considering high concentration [37], Auger model and Lombardi (CVT) Model [38] have been ultilized for simulation of V-siNWTFET device.

3 Results and Analysis

The simulation of Vi-siNWTFET has been carried through Silvaco (ATLAS) Tools. The intial value of relative permittivity (K) of the Biomolecules is taken as 1 in the cavity region. The position when cavity area is filled with bio-logical molecules, the predictable value is increasing from its initial value ($K_{air} = 1$). As per the change in the value K, the bio-logical molecules are immobilized in the cavity area and the electrical properties of the device changes acoordingly. The detail of various bio molecules and their respective relative permittivities are given in Table 2.

3.1 Effect of Neutral Biomolecules on Drain Current

In this section, the effect of neural biomolecules on the drain current has been analyzed with the change in their relative permittivity (K) at $V_{DS} = 1.0$ V as shown in Fig. 3.

Figure 3 shows the variation of drain current with respect to V_{GS} for neutral biomolecules. Initially, it is assumed that the cavity area is filled with air (K = 1), which results in low ON current (I_{ON}). As the cavity area is filled with different biomolecules such as lipids, biotin, uricase, protein, Gox, streptavidin, uriease, zein and immobilized in the cavity by varing their respective relative permittivities from 1.00 to 5.00, resulting increase in I_{ON} current. The detailed of obtained parameters variation of V-siNWTFET for netural biomolecules are given in Table 3.

3.2 Effect of Charge-Biomolecules on Drain Current (I_D)

The effect charged (positive and negative) biomolecules on the drain current with respect to the change in value of K has been analized at $V_{DS} = 1.0$ V as shown in Fig. 4.

The position when carvity area is filled with Zein biomolecules (K = 5.00) and positively chargered biomolecules are immobilized in the cavity area via change in surface density (N_f), then corresponding threshold voltage (V_{th}) start reduces with the increase in surface densities from $N_f = 3e11$ to $N_f = 3e12$ as shown in Fig. 4(a). Similary when cavity is filled with negatively charged biological molecules via $N_f = -3e11$ to $N_f = -3e12$ and immobilized in the cavity region, then the reverse action has been performed and threshold voltage (V_{th}) start increasing with the increase in negatively chargered biomolecules as shown in Fig. 4(b).

Table 1 Device parameters of V-siNWTFET

Parameters	Symbol	Applied values
Channel/Gate Length	L_{gate}	50 nm
Gate-metal Workfunction	Φ_{gate}	4.8 eV
Length of Cavity Region	L_{cavity}	35 nm
Thickness of gate oxide	T_{ox}	2.0 nm
Radius of Nanowire	R_{NW}	10 nm
Thickness of cavity area	T_{cavity}	2.0 nm
Doping Concentration	N_D	1×10^{19} cm^{-3}
Source-metal Workfunction	ϕ_{sorce}	5.93 eV
Drain/Source Length	L_{source}/L_{drain}	50 nm

Table 2 Biological molecules with their respective relative permittivity

Biological molecule	Relative permittivity (K)	Reference
Uricase	1.54	[3]
Uriease	1.64	[1]
Lipids	2.00	[1]
Streptavidin	2.10	[2]
Protein	2.50	[2]
Biotin	2.63	[1]
Gox	3.46	[4]
Zein	5.00	[5]

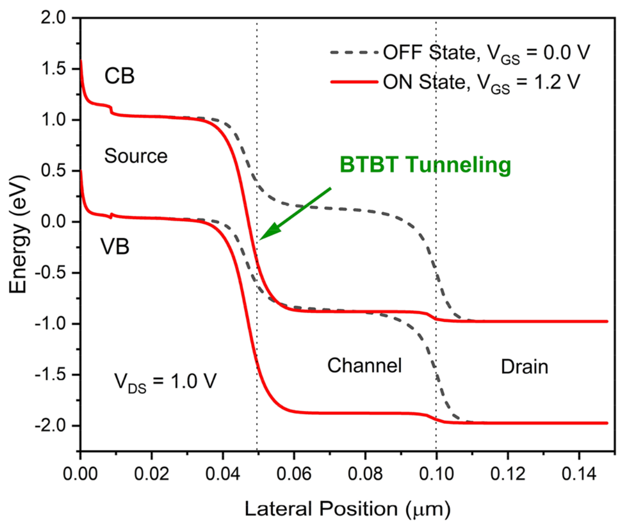

Fig. 2 Engery bands diagram of V-siNWTFET in OFF state ($V_{GS}=0.0$ V) and ON State ($V_{GS}=1.2$ V) at $V_{DS}=1.0$ V

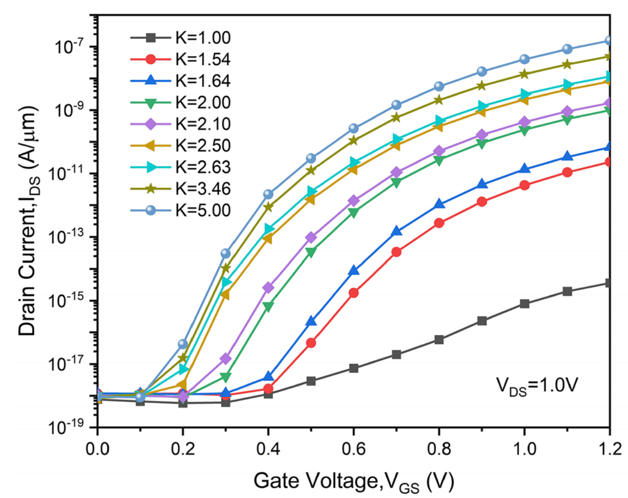

Fig.3 Improvement in I_{ON} current with increased dielectric constant (K) of neutral biomolues at $V_{DS}=0.8$ V

The resultant parameters variation of V-siNWTFET after the simulation for charged Biomolecules with K = 5.00 are given in Table 4.

3.3 Effect on Engery Bands of V-siNWTFET with respect to different biomolecules

In this section the effect of different neutral biomolucules on engery bands have been considered in OFF-state and On-state at $V_{DS}=1.0$ V as shown in Fig. 5. According to the engery band diagram, dash line shows the OFF-state ($V_{GS}=0.0$ V and $V_{DS}=1.0$ V) and solid line shows the ON-state($V_{GS}=1.0$ V and $V_{DS}=1.0$ V). When biomolecules are starts entering into the cavity region it affects the energy bandgaps. As per increase in relative permittivity of the V-siNWTFET from K = 1.64 to K = 5.00 and biological molecules are immobilized in the cavity. The engery gap between the conduction band (CB) and Valance band (VB) has been reduced with the increase in value of K, which results increase in tunneling probability of charge-carrier at the source channel interface of the proposed device.

3.4 Impact on Electric Field for Various Relative Permittivity (K)of the Biomolecules

Figure 6 illustrates the impact on electric field for various relative permittivities of the Biomolecules taken as per Table 2. of V-siNWTFET at $V_{DS}=1.0$ V.

Figure 6 reflects that with the increase in relative permittivity (K) from 1.00 to 5.00, the electric field has been increases. The maximum electric field is observed near source-channel interface (where the tunneling process has been performed) at K = 5.00.

Table 3 Parameter variations of V-siNWTFET for neutral biomolecules

Relative permittivity (K)	I_{ON} (A/μm)	I_{OFF} (A/μm)	I_{ON}/I_{OFF} Ratio	SS (mV/dec)
1.00	1.96E−15	8.53E−19	2.30E+03	86.9025
1.54	4.26E−12	1.18E−18	3.61E+06	63.5005
1.64	1.36E−11	1.19E−18	1.15E+07	57.4164
2.00	2.42E−10	1.02E−18	2.38E+08	44.8274
2.10	4.25E−10	1.04E−18	4.10E+08	44.6145
2.50	2.17E−09	8.30E−19	2.62E+09	36.7055
2.63	3.17E−09	9.05E−19	3.50E+09	36.3842
3.46	1.37E−08	9.44E−19	1.45E+10	35.2091
5.00	4.00E−08	9.34E−19	4.29E+10	31.7323

3.5 Effect of Biomolecules on Drain Current Sensitivity for V-siNWTFET

The effect of biomolecules on drain crurrent sensitivity with $T_{cavity} = 2$ nm at $V_{DS} = 1.8$ V shows in Fig. 7. The Drain Current Sensitivity (ψ_{Id}) of the proposed device is computed through the Eq. (3).

$$\psi_{Id}(\%) = \left[\left(\frac{(\psi_{bio} - \psi_{air})}{\psi_{air}}\right) * 100\right] \quad (3)$$

whereas the ψ_{air} is represents the drain current when the cavity is filled with air and ψ_{bio} is represents the drain current when entire cavity filled with biomolecules [39].

At the intial stage, entire cavity is filled with air (K = 1) and with the increases the K from 1.54 to 5.00, the Drain Current Sensitivity (ψ_{Id}) siginificently improved by taking air as reference material of the cavity region. It is noted that higher percentage ψ_{Id} is observed for Zein Biomolecules having relative permittivity is equal to 5.

3.6 Impact on Transconductance and their Sensitivity for Various K of Biomolecules

In this section the impact of neutral biomolecules on transconductance and their sensitivity has been analyzed as shown in Fig. 8. In general the transconductance of a device is defined as the ratio of change in output current (I_{out}) to the change in input voltage (V_{in}), it is represents as g_m [40]. The mathematical expression for transconductance is given in Eq. (4)

$$\text{Transconductance}\left(g_m\right) = \frac{\Delta I_{out}}{\Delta V_{in}} \quad (4)$$

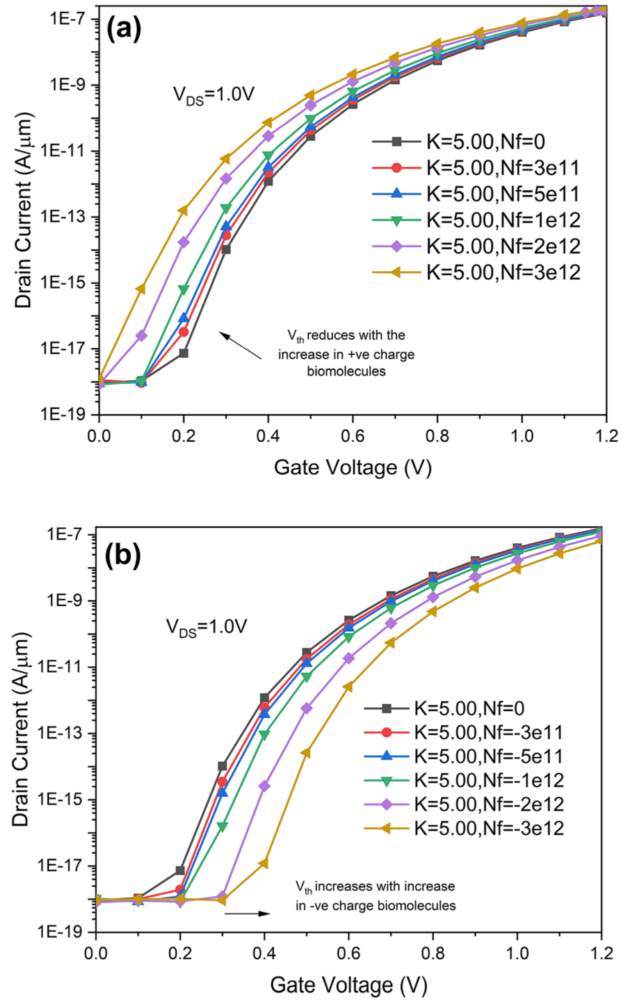

Fig. 4 Effect of charged biomolecules on drain current **a** Positive charged **b** Negative charged biomolucules at $V_{DS} = 1.0$ V

From Fig. 8, it is observed that the transconductance is increase with the filling of higher dielectric constant in the cavity region. The dielectric constant netural biomoles varies from greater than air dielectric constant i.e. K = 1 to higher K = 5.00. The higher value is obtained at Zein Biomoecules by taking the relative permittivity is 5.00 as shown in Fig. 8(a).

The Transconductance Sensitivity (ψ_{gm}) is illustrated in Fig. 8(b). The sensitivity of the V-siNWTFET for Biosensor application is measured through the expression given in Eq. (5).

Table 4 Parameter variations of V-siNWTFET for positive and negative charged biomolecules

Surface Density (Nf)	SS (mV/dec)	I_{ON} (A/μm)	I_{OFF} (A/μm)	I_{ON}/I_{OFF} Ratio	V_{th} (V)
+3e11	34.1302	4.42E−08	1.14E−18	3.88E+10	0.477755
+5e11	35.8853	4.70E−08	9.01E−19	5.22E+10	0.47431
+1e12	35.7079	5.41E−08	8.33E−19	6.49E+10	0.465431
+2e12	35.2652	6.74E−08	8.44E−19	7.99E+10	0.442185
+3e12	36.5971	7.75E−08	1.24E−18	6.27E+10	0.425869
−3e11	30.7042	3.60E−08	8.40E−19	4.29E+10	0.487768
−5e11	32.1401	3.34E−08	9.98E−19	3.35E+10	0.490996
−1e12	36.1484	2.73E−08	1.04E−18	2.62E+10	0.498844
−2e12	29.9879	1.69E−08	8.10E−19	2.09E+10	0.513722
−3e12	29.972	9.40E−09	9.62E−19	9.78E+09	0.527644

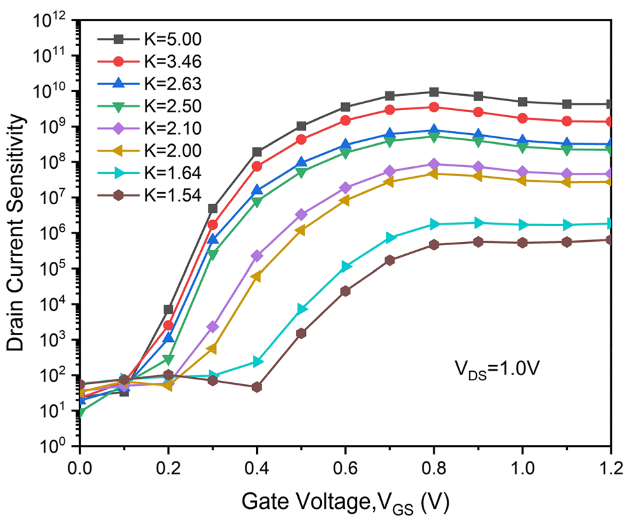

Fig. 7 Effect of neutral biomolecules on drain current sensitivity at $T_{cavity}=2$ nm, $L_{cavity}=35$ nm and $V_{DS}=1.0$

$$\psi_{gm}(\%) = \left[\left(\frac{(g_{mbio} - g_{mair})}{g_{mair}}\right) * 100\right] \quad (5)$$

whereas g_{mbio} and g_{mair} represents as transconductance of bio-logical molecules and air respectively. Figure 8(b) deplicts the absolute value of ψ_{gm} by the variation in cavity filling with different bio-logical molecules. The sensitivity of the V-siNWTFET can be increases or decreases as per the cavity materials such Uricase (K=1.54), Uriease (1.64), Lipids (K=2.00), Streptavidin (K=2.10), Protein (K=2.50), Biotin (K=2.63), Gox (3.46), Zein (K=5.00). From Fig. 8(b), it is evident that lower transconductance sensitivity (ψ_{gm}) of the device are observed at K=1.54 and higher ψ_{gm} at K=5.00.

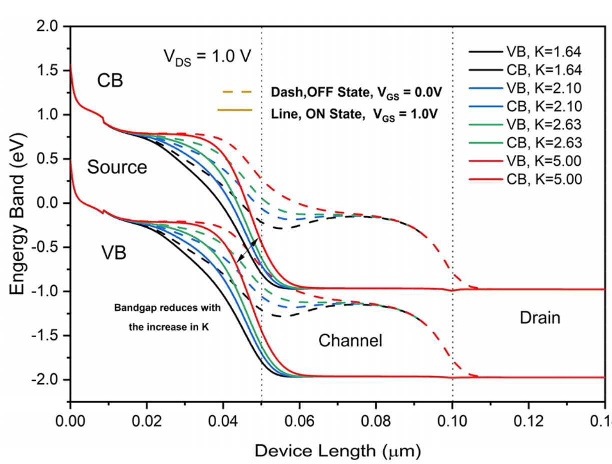

Fig. 5 Variation of energy bands with respect to channel for neutral Biomolecules varies from K=1.64 to 5.00 at $V_{DS}=1.0$ V

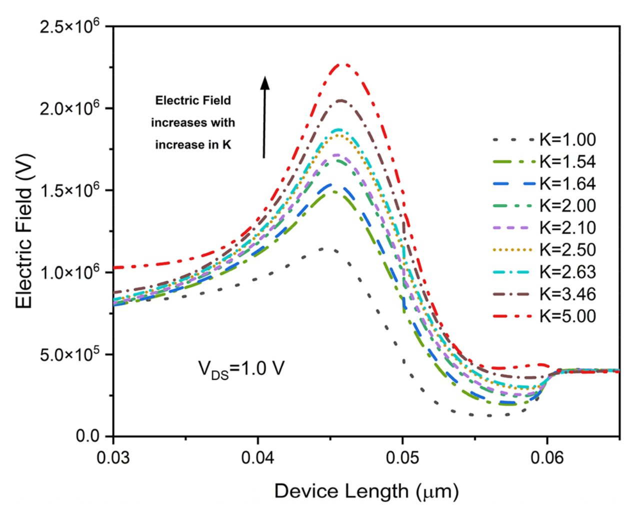

Fig. 6 Impact on electric field for various K at $V_{DS}=1.0$ V

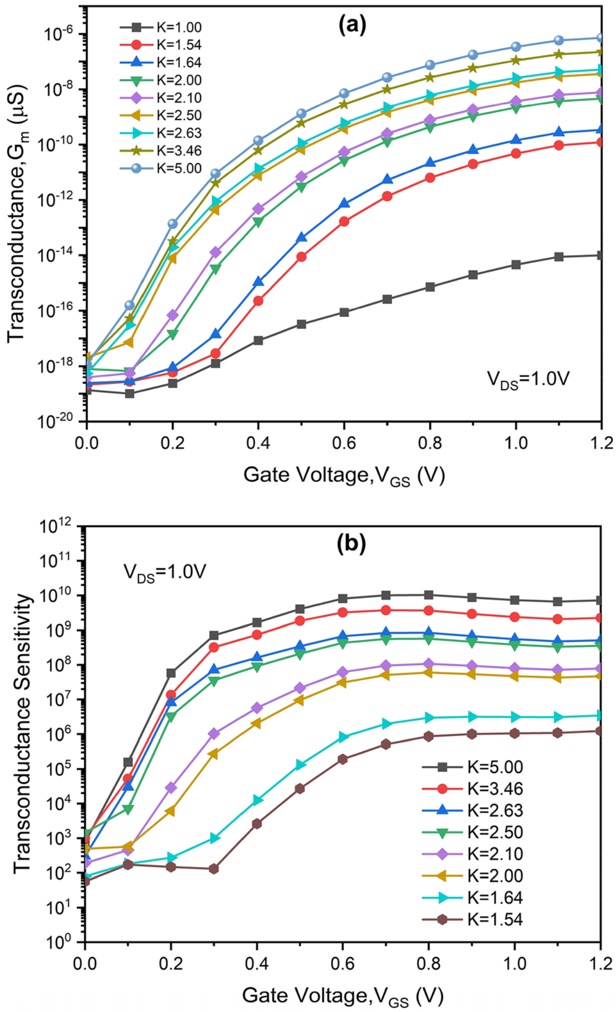

Fig. 8 Effect of Biomolecules **a** Transconductance (g_m) and transconductance sensitivity (ψ_{gm}) at $V_{DS} = 0.8$ V

4 Conclusion

This article presented a V-siNWTFET structure for Biosensor applications by considering its performance analysis using dielectric modulation (DM) technique. The Biomolecules are immobilized in the cavity region by varying the relative permittivities (K). The V-siNWTFET presents the suitable high performance biosensor for detection of biomolecules like u Uricase, Uriease, Lipids, Streptavidin, Protein, Biotin, Gox, Zein etc. The sensitivity of the proposed biosensor has been increases with the increase in dielectric contant in the cavity area by taking air (K = 1) as reference value. The resultant maximum I_{ON} (1.00×10^{-8}), minimum I_{OFF} current (8.31×10^{-19}) and minimum value of I_{ON}/I_{OFF} Ratio (1.21×10^{10}) are observed at K = 5.00. Further the device is optimized for best possible results at $\Phi_{gate} = 4.8$ eV, $L_{cavity} = 35$ nm, $T_{ox} = 2$ nm, Tcavity = 2 nm and $N_D = 1 \times 10^{-19}$ cm^{-3}, and $R_{NW} = 10$ nm. The proposed device also investigates the performance assessment with the impact of neutral as well as charged biomolecule, resulting in low leakage currents, enhanced parametric values and high sensitivity with neutral Biomolecules as compared to other FET based sensor devices. The designed V-siNWT-FET device has been suitable for high performance, energy efficient and high sensitivity biosensor design applications.

Acknowledgements We thank the ECE Department of Dr. B.R. Ambedkar National Institute of Technology,Jalandhar and National Institute of Technical Teachers Training and Research, for their attentiveness in this work and useful comments to draft the final form of the paper. The support of Science and Engineering Research Board (SERB), Government of India (GoI), Project (EEQ/2018/000444) is appreciatively acknowledged. We would like to thank NIT Jalandhar and NITTTR Chandigarh for lab facilities and research environment to carry out this work.

Author Contributions We has been proposed Vertical Silicon Nanowire Tunnel-Field Effect Transistor (V-siNWTFET), which are immune to short channel effects and preferred for high performance biosensor design applications in nano regime.

Funding The authors declare that they have no funding available for the publication chargers of open access. We have received financial support from Science and Engineering Research Board, Government of India for computation and simulation tools to carry out the proposed work.

Declarations

Conflict of interest The proposed device has been suitalble for biosensor applications with reduced short channel effects and improved performance parameters as compared to previous reported work. Authors declare that there is no conflict of Interest.

References

1. A. Paliwal, M. Tomar, V. Gupta, Complex dielectric constant of various biomolecules as a function of wavelength using surface plasmon resonance. J. Appl. Phys. **116**(2), 23109 (2014)
2. A. Densmore et al., Spiral-path high-sensitivity silicon photonic wire molecular sensor with temperature-independent response. Opt. Lett. **33**(6), 596–598 (2008)
3. G. Wadhwa, B. Raj, Parametric variation analysis of symmetric double gate charge plasma JLTFET for biosensor application. IEEE Sens. J. **18**(15), 6070–6077 (2018)
4. S.K. Verma, S. Singh, G. Wadhwa, B. Raj, Detection of biomolecules using charge-plasma based gate underlap dielectric modulated dopingless TFET. Trans. Electr. Electron. Mater. **21**(5), 528–535 (2020)
5. P. Kaur, A. S. Buttar, and B. Raj, "Design and Performance Analysis of Proposed Biosensor based on Double Gate Junctionless Transistor," *Silicon*, pp. 1–8, 2021
6. M. Sheikhshoaie, H. Karimi-Maleh, I. Sheikhshoaie, M. Ranjbar, Voltammetric amplified sensor employing RuO2 nano-road and room temperature ionic liquid for amaranth analysis in food samples. J. Mol. Liq. **229**, 489–494 (2017)

7. M. Stobiecka, S. Jakiela, A. Chalupa, P. Bednarczyk, B. Dworakowska, Mitochondria–based biosensors with piezometric and RELS transduction for potassium uptake and release investigations. Biosens. Bioelectron. **88**, 114–121 (2017)
8. J. Shin, S. Choi, J.-S. Yang, J. Song, J.-S. Choi, H.-I. Jung, Smart Forensic phone: colorimetric analysis of a bloodstain for age estimation using a smartphone. Sens. Actuat. B Chem. **243**, 221–225 (2017)
9. V.-T. Nguyen, Y.S. Kwon, M.B. Gu, Aptamer-based environmental biosensors for small molecule contaminants. Curr. Opin. Biotechnol. **45**, 15–23 (2017)
10. R. Narang, M. Saxena, R.S. Gupta, M. Gupta, Dielectric modulated tunnel field-effect transistor—A biomolecule sensor. IEEE Electron Device Lett. **33**(2), 266–268 (2011)
11. P. Bergveld, Development of an ion-sensitive solid-state device for neurophysiological measurements. IEEE Trans. Biomed. Eng. **1**, 70–71 (1970)
12. A. Bandiziol, P. Palestri, F. Pittino, D. Esseni, L. Selmi, A TCAD-based methodology to model the site-binding charge at ISFET/electrolyte interfaces. IEEE Trans. Electron Devices **62**(10), 3379–3386 (2015)
13. P. Kumar and S. K. Sharma, "Comparative analysis of nanowire tunnel field effect transistor for biosensor applications," *Silicon*, pp. 1–8, 2020
14. A. Gedam, B. Acharya, G.P. Mishra, Design and performance assessment of dielectrically modulated nanotube TFET biosensor. IEEE Sens. J. **21**(15), 16761–16769 (2021)
15. I.C. Cherik, S. Mohammadi, Dielectric modulated doping-less tunnel field-effect transistor, a novel biosensor based on cladding layer concept. IEEE Sens. J. **22**, 10308 (2022)
16. J. Tanaka, T. Toyabe, S. Ihara, S. Kimura, H. Noda, K. Itoh, Simulation of sub-0.1-mu m MOSFETs with completely suppressed short-channel effect. IEEE Electron Device Lett. **14**(8), 396–399 (1993)
17. C. Duvvury, A guide to short-channel effects in MOSFETs. IEEE Circuits Devices Mag. **2**(6), 6–10 (1986)
18. P.-H. Bricout, E. Dubois, Short-channel effect immunity and current capability of sub-0.1-micron MOSFET's using a recessed channel. IEEE Trans. Electron Devices **43**(8), 1251–1255 (1996)
19. S.L. Tripathi, R. Mishra, R.A. Mishra, Multi-gate MOSFET structures with high-k dielectric materials. J. Electron Devices **16**, 1388–1394 (2012)
20. S. Kumar, S. Kumar, K. Kumar, B. Raj, Analysis of double gate dual material tunnel FET device for low power SRAM cell design. Quantum Matter **5**(6), 762–766 (2016)
21. S.L. Tripathi, G.S. Patel, Design of low power Si 0.7 Ge 0.3 pocket junction-less tunnel FET using below 5 nm technology. Wirel. Pers. Commun. **111**(4), 2167–2176 (2020)
22. G. Wadhwa, B. Raj, Surface potential modeling and simulation analysis of dopingless TFET biosensor. SILICON **14**(5), 2147–2156 (2022)
23. B. Ghosh, M.W. Akram, Junctionless tunnel field effect transistor. IEEE Electron Device Lett. **34**(5), 584–586 (2013)
24. S.O. Koswatta, M.S. Lundstrom, D.E. Nikonov, Performance comparison between pin tunneling transistors and conventional MOSFETs. IEEE Trans. Electron Devices **56**(3), 456–465 (2009)
25. J.C. Shin et al., Heterogeneous integration of InGaAs nanowires on the rear surface of Si solar cells for efficiency enhancement. ACS Nano **6**(12), 11074–11079 (2012)
26. B. Jena, K.P. Pradhan, P.K. Sahu, S. Dash, G.P. Mishra, S.K. Mohapatra, Investigation on cylindrical gate all around (GAA) to nanowire MOSFET for circuit application. Facta Univ. Ser. Electron. Energ. **28**(4), 637–643 (2015)
27. G.V. Luong et al., Complementary strained Si GAA nanowire TFET inverter with suppressed ambipolarity. IEEE Electron Device Lett. **37**(8), 950–953 (2016)
28. M.J. Kumar, K. Nadda, Bipolar charge-plasma transistor: a novel three terminal device. IEEE Trans. Electron Devices **59**(4), 962–967 (2012)
29. G. Wadhwa, B. Raj, Label free detection of biomolecules using charge-plasma-based gate underlap dielectric modulated junctionless TFET. J. Electron. Mater. **47**(8), 4683–4693 (2018)
30. Z.X. Chen et al., Demonstration of tunneling FETs based on highly scalable vertical silicon nanowires. IEEE Electron Device Lett. **30**(7), 754–756 (2009)
31. A. Raj, S. Singh, K.N. Priyadarshani, R. Arya, A. Naugarhiya, Vertically extended drain double gate Si1− xGex source tunnel FET: proposal & investigation for optimized device performance. SILICON **13**(8), 2589–2604 (2021)
32. K.N. Priyadarshani, S. Singh, Ultra sensitive label-free detection of biomolecules using vertically extended drain double gate $Si_{0.5}Ge_{0.5}$ source tunnel FET. IEEE Trans. Nanobiosci. **20**(4), 480–487 (2021)
33. G. Wadhwa, B. Raj, Design, simulation and performance analysis of JLTFET biosensor for high sensitivity. IEEE Trans. Nanotechnol. **18**, 567–574 (2019)
34. T. Goudon, V. Miljanović, C. Schmeiser, On the shockley–read–hall model: generation-recombination in semiconductors. SIAM J. Appl. Math. **67**(4), 1183–1201 (2007)
35. S. Sahay, M.J. Kumar, Insight into lateral band-to-band-tunneling in nanowire junctionless FETs. IEEE Trans. Electron Devices **63**(10), 4138–4142 (2016)
36. R. Narang, M. Saxena, M. Gupta, Comparative analysis of dielectric-modulated FET and TFET-based biosensor. IEEE Trans. Nanotechnol. **14**(3), 427–435 (2015)
37. J.W. Slotboom, H.C. De Graaff, Bandgap narrowing in silicon bipolar transistors. IEEE Trans. Electron Devices **24**(8), 1123–1125 (1977)
38. C. Lombardi, S. Manzini, A. Saporito, M. Vanzi, A physically based mobility model for numerical simulation of nonplanar devices. IEEE Trans. Comput. Des. Integr. Circuits Syst. **7**(11), 1164–1171 (1988)
39. D. Singh, S. Pandey, K. Nigam, D. Sharma, D.S. Yadav, P. Kondekar, A charge-plasma-based dielectric-modulated junctionless TFET for biosensor label-free detection. IEEE Trans. Electron Devices **64**(1), 271–278 (2016)
40. L. Barboni, M. Siniscalchi, B. Sensale-Rodriguez, TFET-based circuit design using the transconductance generation efficiency ${g} _ m}/{I _ d $ method. IEEE J. Electron Devices Soc. **3**(3), 208–216 (2015)

Publisher's Note Springer Nature remains neutral with regard to jurisdictional claims in published maps and institutional affiliations.